Chaotic dynamics and basin erosion in nanomagnets subject to time-harmonic magnetic fields

Chaotic dynamics and basin erosion in nanomagnets subject to time-harmonic magnetic fields

M. d'Aquino [a], A. Quercia [b], C. Serpico [b], G. Bertotti [c], I.D. Mayergoyz [d], S. Perna [a], P. Ansalone [b]

[a] *Engineering Department, University of Naples "Parthenope", 80143 Naples, Italy* [b] *DIETI, University of Naples Federico II, 80125 Naples, Italy*
[c] *Istituto Nazionale di Ricerca Metrologica, 10135 Torino, Italy*
[d] *ECE Department and UMIACS, University of Maryland, College Park, MD 20742, USA*

ABSTRACT

Magnetization dynamics in uniformly magnetized particles subject to time-harmonic (AC) external fields is considered. The study is focused on the behavior of the AC-driven dynamics close to saddle equilibria. It happens that such dynamics has chaotic nature at moderately low power level, due to the heteroclinic tangle phenomenon which is produced by the combined effect of AC-excitations and saddle type dy-namics. By using analytical theory for the threshold AC excitation amplitudes necessary to create the heteroclinic tangle together with numerical simulations, we quantify and show how the tangle produces the erosion of the safe basin around the stable equilibria.

Keywords:
Landau–Lifshitz equation Chaotic dynamics Heteroclinic tangle Basin erosion Fractal basin boundaries

Magnetization dynamics in uniformly magnetized nanomagnets subject to time-harmonic (AC) fields has been traditionally studied in connection with ferromagnetic resonance [1]. In this situation, AC fields produce small magnetization oscillations around a stable equilibrium and the response of the system depends on the frequency of the excitation following, in the linear regime, the classical resonance curve peaked around the Kittel frequency [2]. Since magnetization dynamics is usually weakly dissipative, nonlinear effects can be excited at moderately large powers, which can give rise to hysteretic (bistable) resonance response owing to the fold-over effect [3].

In this paper, we investigate the effects of time-harmonic external fields in a wider region of the state space. In particular, we are interested in the regions around saddle-type equilibria which are usually at the top of the potential wells. The motivation for studying such an unstable region is connected with the fact that saddle equilibria and the associated heteroclinic/homoclinic manifolds connecting the saddles, usually termed separatrices, constitute the boundaries of basins of attraction of different attractors (asymptotic regimes). It turns out that the AC perturbations of the dynamics in the vicinity of saddle equilibria give rise to phenomena incomparably more complex than those observed close to a stable equilibrium.

These complex phenomena are due to the possibility that the homoclinic/heteroclinic manifolds, for sufficiently large AC excitations, may intersect infinitely many times forming a structure referred to as homoclinic/heteroclinic tangle which may lead to separatrices which have a fractal geometrical nature. As a con-

sequence, the magnetization dynamics starting inside an energy well may, at later time, escape the well. This mechanism is called basin erosion and starts in the vicinity of the saddle equilibria and the associated homoclinic/heteroclinic cycles [4].

The purpose of this paper is to investigate the connection between the aforementioned tangling phenomena and basin erosion for magnetization dynamics driven by AC external fields. In the paper, magnetization dynamics is described by the Landau–Lifshitz (LL) equation. The external field is assumed to be purely sinusoidal with no bias. In these conditions, the entanglement of saddle manifolds is of the heteroclinic type. The origin of heteroclinic tangle is first illustrated from the qualitative point of view. Then, by using analytical formulas based on Melnikov function [5] to characterize AC field amplitudes for the onset of the heteroclinic tangle, we perform numerical simulations of the AC-driven magnetization dynamics suitable to introduce a measure for the phenomenon of basin erosion. Finally, some remarks on the connection between basin erosion and microwave-assisted magnetization switching are given.

The evolution of the magnetization $\boldsymbol{M}$ in a uniformly magnetized particle is described in terms of normalized vector $\boldsymbol{m} = \boldsymbol{M}/M_s$, where M_s is the saturation magnetization and $|\boldsymbol{m}| = 1$. The evolution of $\boldsymbol{m}$ on the unit sphere Σ is governed by the following generalized Landau–Lifshitz equation [6]:

$$\frac{d\boldsymbol{m}}{dt} = \boldsymbol{m} \times \nabla_\Sigma g - \alpha \nabla_\Sigma g, \tag{1}$$

where ∇_Σ is the gradient operator on the unit sphere, $g = g(\boldsymbol{m}, t)$ is the free energy and α is the damping. We use normalized quantities so that time is measured in units of $(\gamma M_s)^{-1}$, (γ is the gyromagnetic ratio), and the energy function g in units of $\mu_0 M_s^2 V$ (μ_0 is the vacuum permeability and V the volume of the particle). The free energy is given by the following expression:

$$g(\boldsymbol{m}, t) = g_0(\boldsymbol{m}) - \boldsymbol{h}_{ac}(t)\cdot\boldsymbol{m}, \tag{2}$$

where

$$g_0(\boldsymbol{m}) = (D_x m_x^2 + D_y m_y^2 + D_z m_z^2)/2, \tag{3}$$

D_x, D_y, D_z are effective anisotropy constants. The field $\boldsymbol{h}_{ac}(t)$ in Eq. (2) is the time-harmonic (AC) external field

$$\boldsymbol{h}_{ac}(t) = \mathbf{e}_x h_{ax}\cos(\omega t + \delta_x) + \mathbf{e}_y h_{ay}\cos(\omega t + \delta_y) + \mathbf{e}_z h_{az}\cos(\omega t + \delta_z), \tag{4}$$

where $\mathbf{e}_x$, $\mathbf{e}_y$, $\mathbf{e}_z$ are the cartesian unit vectors, and where h_{ax}, h_{ay}, h_{az}, δ_x, δ_y, δ_z are the amplitudes and phases of the cartesian components of $\boldsymbol{h}_{ac}(t)$, respectively.

In most situations of practical and physical interest, it happens that α, $h_{ac} \ll 1$ ($h_{ac} = \sqrt{h_{ax}^2 + h_{ay}^2 + h_{az}^2}$). This leads to the following perturbative form of Eq. (1):

$$\frac{\mathrm{d}\boldsymbol{m}}{\mathrm{d}t} = \boldsymbol{v}_0(\boldsymbol{m}) + \varepsilon\boldsymbol{v}_1(\boldsymbol{m}, t) = \boldsymbol{v}(\boldsymbol{m}, t, \varepsilon), \tag{5}$$

where $\boldsymbol{v}_0(\boldsymbol{m}) = \boldsymbol{m} \times \nabla_\Sigma g_0(\boldsymbol{m})$ is the unperturbed Hamiltonian vector field and $\varepsilon\boldsymbol{v}_1(\boldsymbol{m}, t) = -\boldsymbol{m} \times \boldsymbol{h}_{ac}(t) - \alpha\nabla_\Sigma g(\boldsymbol{m}, t)$. The parameter ε is formally introduced in preparation of a perturbation analysis of the dynamics based on the assumption that $\varepsilon \ll 1$. One can interpret ε as a parameter which controls the amplitude of all small quantities in the problem, and more specifically, the amplitude of AC excitations. In the form (5), the equation governing magnetization dynamics is a perturbed Hamiltonian dynamics on the unit sphere with Hamiltonian given by the function $g_0(\boldsymbol{m})$.

The non-autonomous dynamical system (5) can be analyzed by introducing the stroboscopic map [7]:

$$\boldsymbol{m}_{n+1} = P[\boldsymbol{m}_n, \varepsilon], \tag{6}$$

where $\boldsymbol{m}_n = \boldsymbol{m}(t_0 + nT)$, and $T = 2\pi/\omega$, which maps an initial magnetization $\boldsymbol{m}(t_0)$ to the magnetization $\boldsymbol{m}(t_0 + T)$ obtained by integrating Eq. (5), over a time interval equal to T. Notice that the stroboscopic map (6) is a time-discrete dynamical system and thus its trajectories are sequence of points on Σ. Analytical treatment of $P[\cdot]$ is based on the following Taylor expansion:

$$P[\mathbf{m}_n, \varepsilon] = P[\mathbf{m}_n, 0] + \frac{\partial P}{\partial \varepsilon}[\mathbf{m}_n, 0]\varepsilon + O(\varepsilon^2). \tag{7}$$

The zero order term of the expansion gives the unperturbed map whose trajectories are curves with constant value of $g_0(\boldsymbol{m})$ which can be determined in closed form [6]. This implies that the saddles of the unperturbed map $P[\mathbf{m}_n, 0]$ coincide with the saddle equilibria associated with the vector field $\boldsymbol{v}_0(\boldsymbol{m})$. The qualitative features of the phase portrait of $\boldsymbol{v}_0(\boldsymbol{m})$ are represented in Fig. 1(a) in cylindrical coordinates (ϕ, m_z). The two saddles $\boldsymbol{x}_{d1}$ and $\boldsymbol{x}_{d2}$ are connected through heteroclinic trajectories, which are invariant sets of the map $P[\mathbf{m}_n, 0]$. We recall that an invariant set A of a map $P[\cdot]$ is such that $P[A] \subseteq A$. Heteroclinic trajectories are typical only in conservative systems and they are not structurally stable with respect to generic perturbation of the system. For this reason, they

a

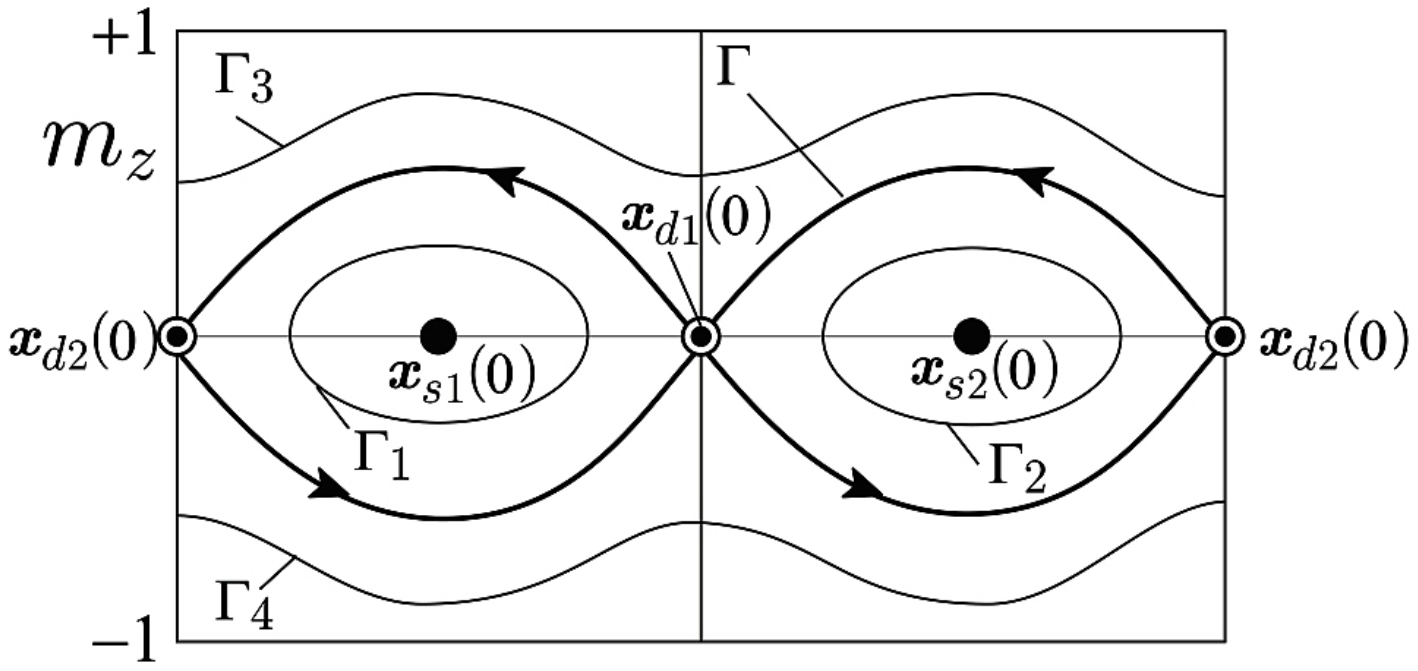
+1
m_z
Γ_3
Γ
$x_{d1}(0)$
$x_{d2}(0)$
$x_{s1}(0)$
$x_{s2}(0)$
$x_{d2}(0)$
Γ_1
Γ_2
Γ_4
−1

b

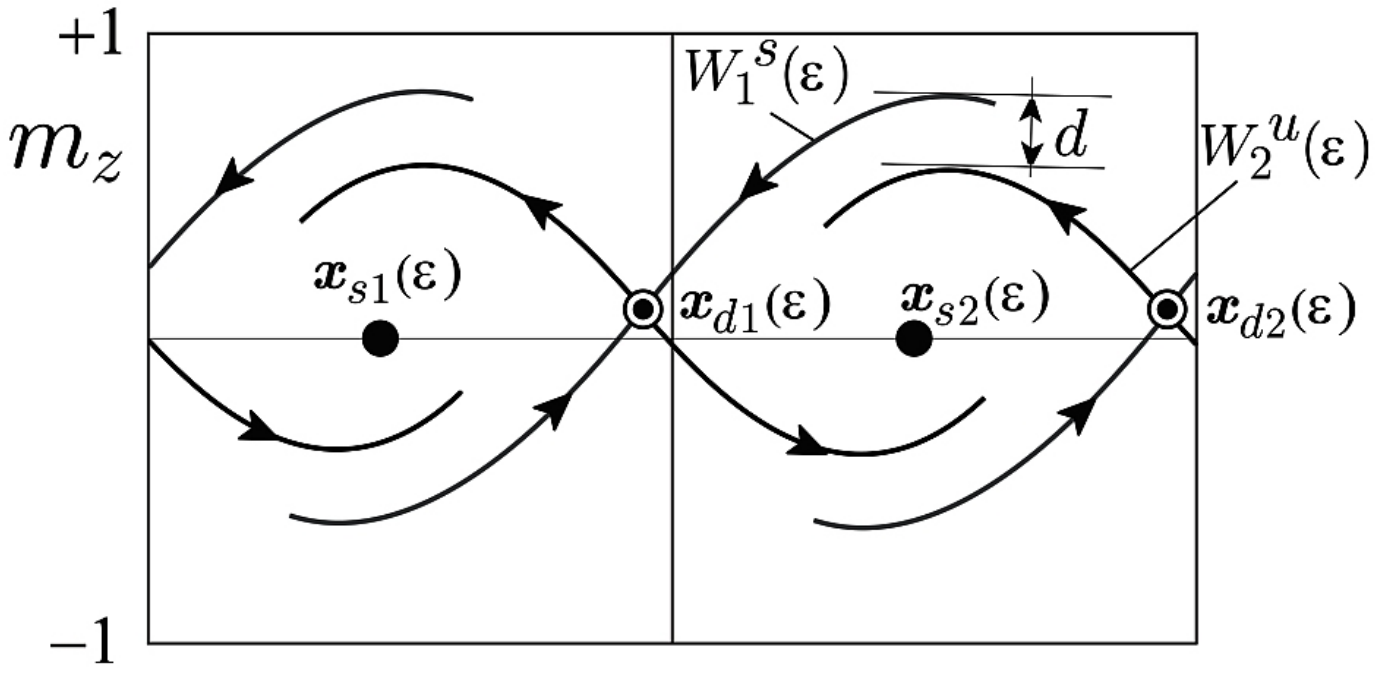
+1
m_z
$W_1^s(\varepsilon)$
d
$W_2^u(\varepsilon)$
$x_{s1}(\varepsilon)$
$x_{d1}(\varepsilon)$
$x_{s2}(\varepsilon)$
$x_{d2}(\varepsilon)$
−1

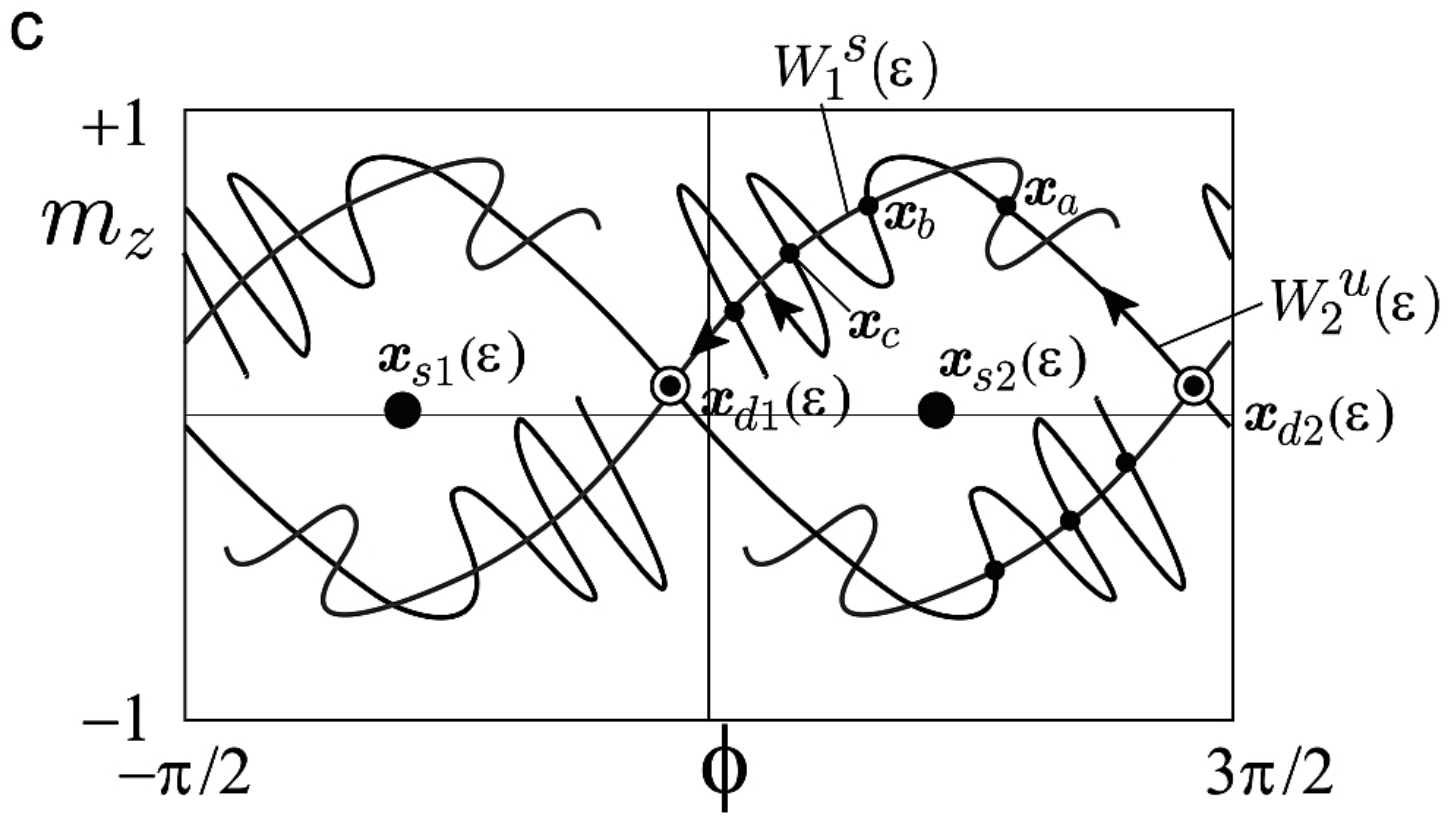

Fig. 1. Qualitative sketches of the separatrices associated to the stroboscopic map (see Eq. (6)) in the (ϕ, m_z)-plane (where ϕ is the azimuth around the z-axis). (a) Unperturbed case; (b) damping dominated dynamics; and (c) heteroclinic tangle formation. Legend: $\boldsymbol{x}_{d1}(\varepsilon)$, $\boldsymbol{x}_{d2}(\varepsilon)$ saddle equilibria; $\boldsymbol{x}_{s1}(\varepsilon)$, $\boldsymbol{x}_{s2}(\varepsilon)$ node-type equilibria; $W_1^s(\varepsilon)$ stable manifold associated with $\boldsymbol{x}_{d1}(\varepsilon)$; $W_2^u(\varepsilon)$ unstable manifold associated with $\boldsymbol{x}_{d2}(\varepsilon)$; d splitting of the manifolds; Γ heteroclinic trajectory, and Γ_1, ...Γ_4 constant energy trajectories. The points $\boldsymbol{x}_a$, $\boldsymbol{x}_b$, $\boldsymbol{x}_c$ are generated by iterating the stroboscopic map.

are immediately destroyed when nonconservative perturbations set in. On the other hand, saddle fixed points are structurally stable entities [7] and thus are preserved under small perturbations. In the perturbed case, two invariant curves originate from each saddle of the map: the stable manifold W^s and the unstable manifold W^u [7]. In Fig. 1(b) the two manifolds $W_1^s(\varepsilon)$ and $W_2^u(\varepsilon)$ are sketched and their separation (splitting) is indicated by d. This splitting depends on the nature of perturbation and may vanish for sufficiently large AC perturbations. When this occurs, a point of intersection $\boldsymbol{x}_a$ belonging to both invariant set $W_1^s(\varepsilon)$ and $W_2^u(\varepsilon)$ is

realized (see Fig. 1(c)). This implies that forward and backward iterates of $P[\cdot]$ starting from $\boldsymbol{x}_a$ must belong to $W_1^s(\varepsilon) \cap W_2^u(\varepsilon)$ and thus that the two curves, $W_1^s(\varepsilon)$ and $W_2^u(\varepsilon)$, must intersect an infinite number of times (see Fig. 1(c)). This phenomenon is referred to as heteroclinic tangle and it is at the origin of chaotic and unpredictable dynamic behavior of the system near the saddles. In order to find when this occurs, one must be able to compute the splitting d of $W_1^s(\varepsilon)$ and $W_2^u(\varepsilon)$. By using the expansion (7), the

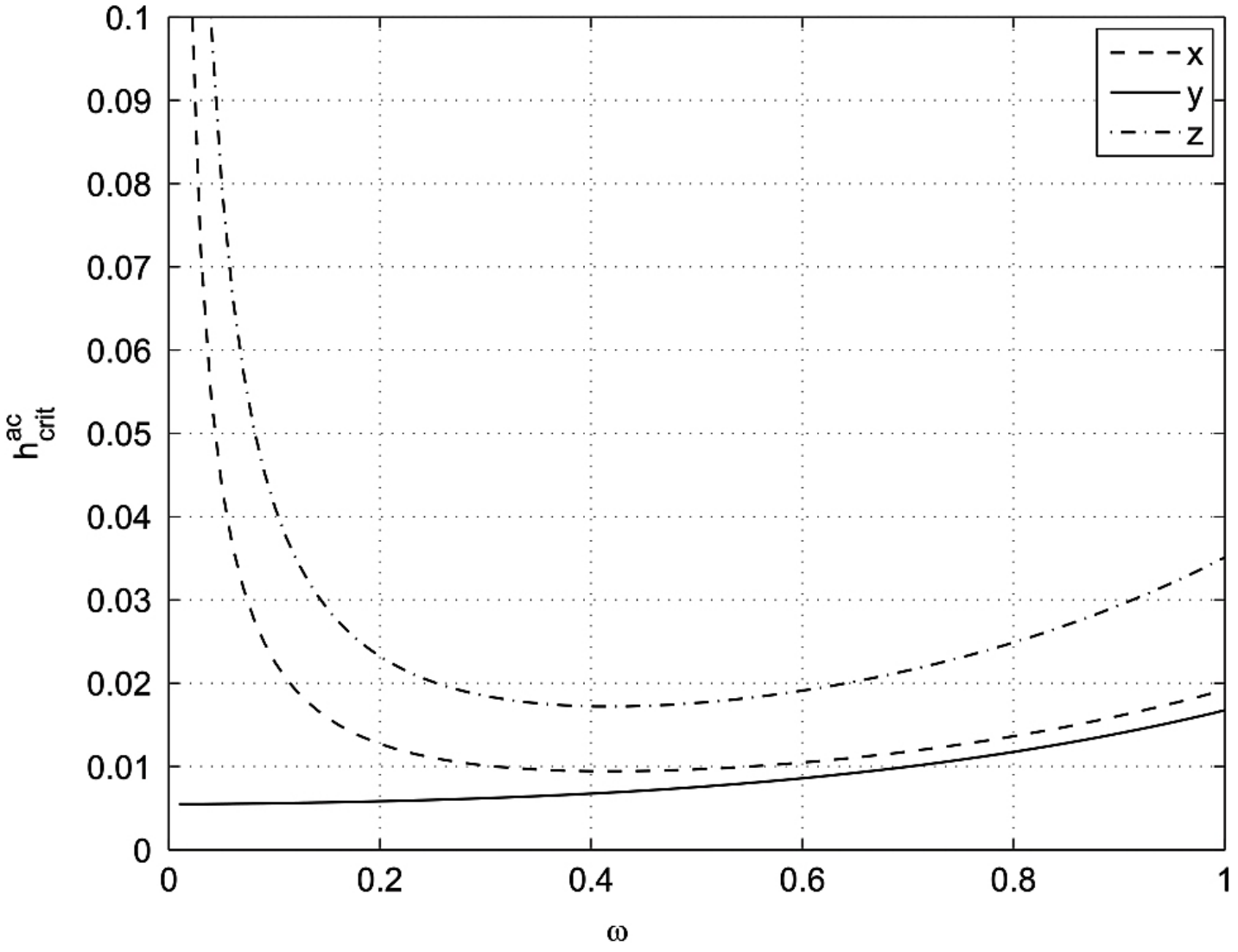

Fig. 2. Threshold values of *ac* fields for creation of heteroclinic tangle versus ω for the various polarizations. Values of parameters: $\alpha = 0.01$, $D_x = -0.3$, $D_y = 0$, and $D_z = 1$.

splitting has been analytically derived [8] and allows one to derive the threshold values for the AC excitation which give rise to the tangling phenomenon.

Such threshold values of h_{ac} for the onset of the heteroclinic tangle, for linear polarization along each of the coordinate axes are, respectively [8]:

$$h_{ac,j}^{\mathrm{crit}} = \frac{2\alpha\Omega_d}{|u_j(\omega)|}, \tag{8}$$

where $j = \{x, y, z\}$, $k^2 = (D_z - D_y)/(D_z - D_x)$, $k'^2 = 1 - k^2$, $\Omega_d = \sqrt{(D_z - D_y)(D_y - D_x)}$, $q = \omega/\Omega_d$ and

$$\boldsymbol{u}(\omega) = (s_x k \boldsymbol{e}_x + s_z k' \boldsymbol{e}_z)\frac{-\mathrm{i}\pi q}{\cosh\dfrac{\pi q}{2}} + s_x s_z \boldsymbol{e}_y \frac{\pi q}{\sinh\dfrac{\pi q}{2}}, \quad s_x,\ s_z = \pm 1. \tag{9}$$

We remark that Eq. (9) corrects a typo present in Ref. [8]. The critical amplitudes predicted by Eq. (8) as function of the angular frequency ω are reported in Fig. 2. They represent the threshold values of *AC* fields for creation of heteroclinic tangle for typical values of the parameters.

A direct and important consequence arising from the onset of the heteroclinic tangle on the magnetization dynamics is the phenomenon of erosion of the basins of attraction. The erosion has important practical effects since it is similar to a reduction of the depth of the potential well and thus it reduces the 'safety region' around a stable equilibrium state. In addition, the boundary of the basin of attraction of asymptotic regimes inside the well acquires a fractal nature. These phenomena might be at the basis of complex features obtained in the measurement of Stoner–Wohlfarth astroid in the presence of microwave fields [9].

Such a phenomenon has been studied numerically by solving

Eq. (1) for an ensemble of very large number N of particle replicas starting from initial conditions filling the energy well around $\boldsymbol{m} = \boldsymbol{e}_x$. In particular, a given number n of iterates of the stroboscopic map (6) has been computed starting from an initial magnetization state $\boldsymbol{m}_0$ such that

$$g(\boldsymbol{m}_0) < g_d = \frac{D_y}{2}, \tag{10}$$

where g_d is the energy associated with the saddle of the unperturbed dynamics.

After each n-iterate, the condition (10) on the energy is checked

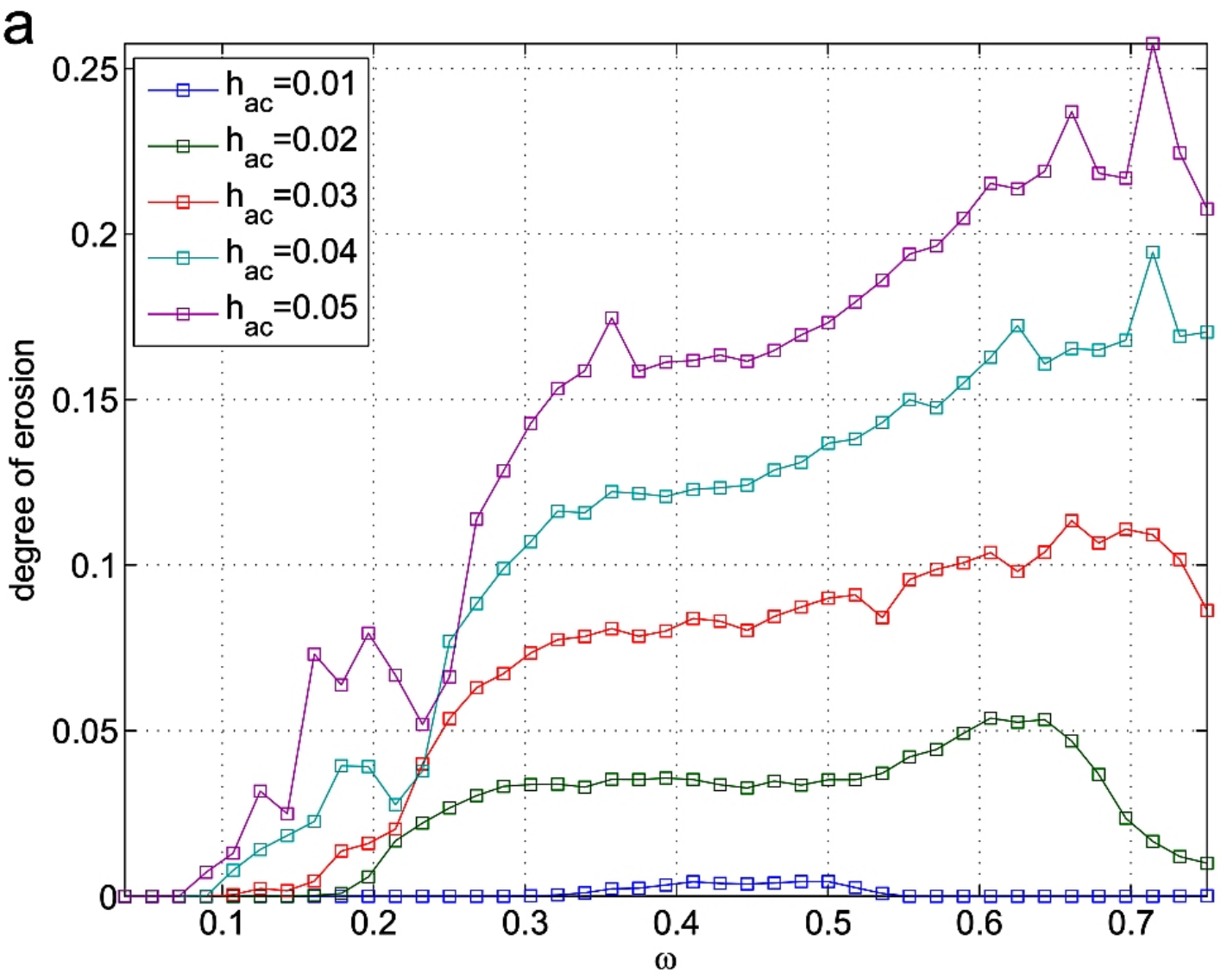

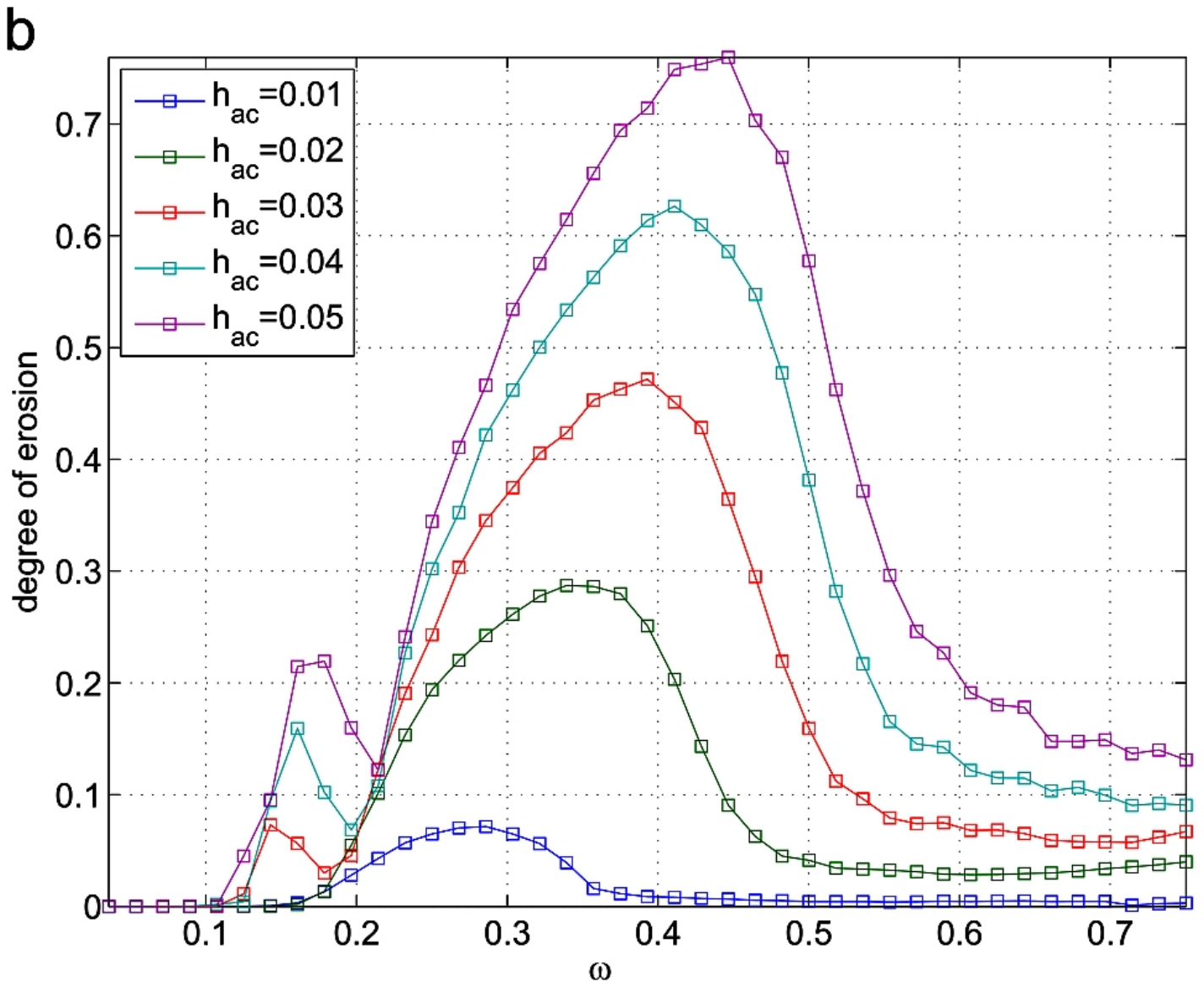
b
h_ac=0.01
h_ac=0.02
h_ac=0.03
h_ac=0.04
h_ac=0.05
degree of erosion
ω
0
0.1
0.2
0.3
0.4
0.5
0.6
0.7

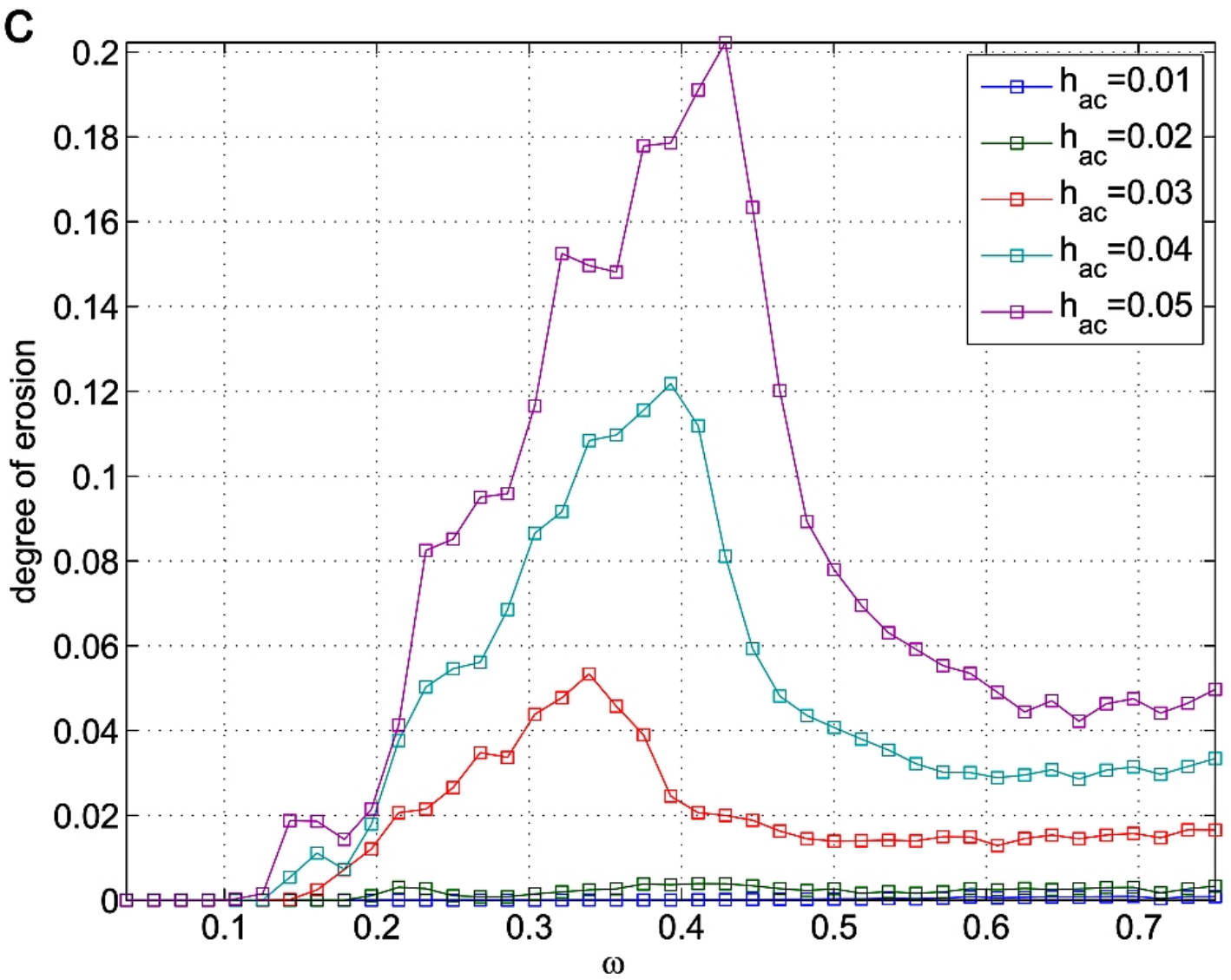

Fig. 3. Degree of basin erosion η as function of frequency ω and AC field amplitude h_{ac} for fields linearly polarized along the direction: (a) x, (b) y, (c) z. In the numerical computations, $N = 10^5$ particle replicas and $n=5$ iterates of the stroboscopic map are considered. Values of parameters: $D_x = -0.3$, $D_y = 0$, $D_z = 1$, and $\alpha = 0.01$.

and then, if it is not fulfilled, the initial condition associated with that particle is removed from the energy well and the number of escaped particles is increased.

As a measure of the strength of the phenomenon, we define the following degree of erosion η:

$$\eta = \frac{\#\text{particle escaped}}{N}. \tag{11}$$

The result of the numerically computed degree of erosion η as function of the angular frequency ω and AC field amplitude h_{ac} is reported in Fig. 3(a)–(c). It has been obtained by solving the LL equation (5) for $N = 10^5$, $n=5$ and linear polarizations of the AC

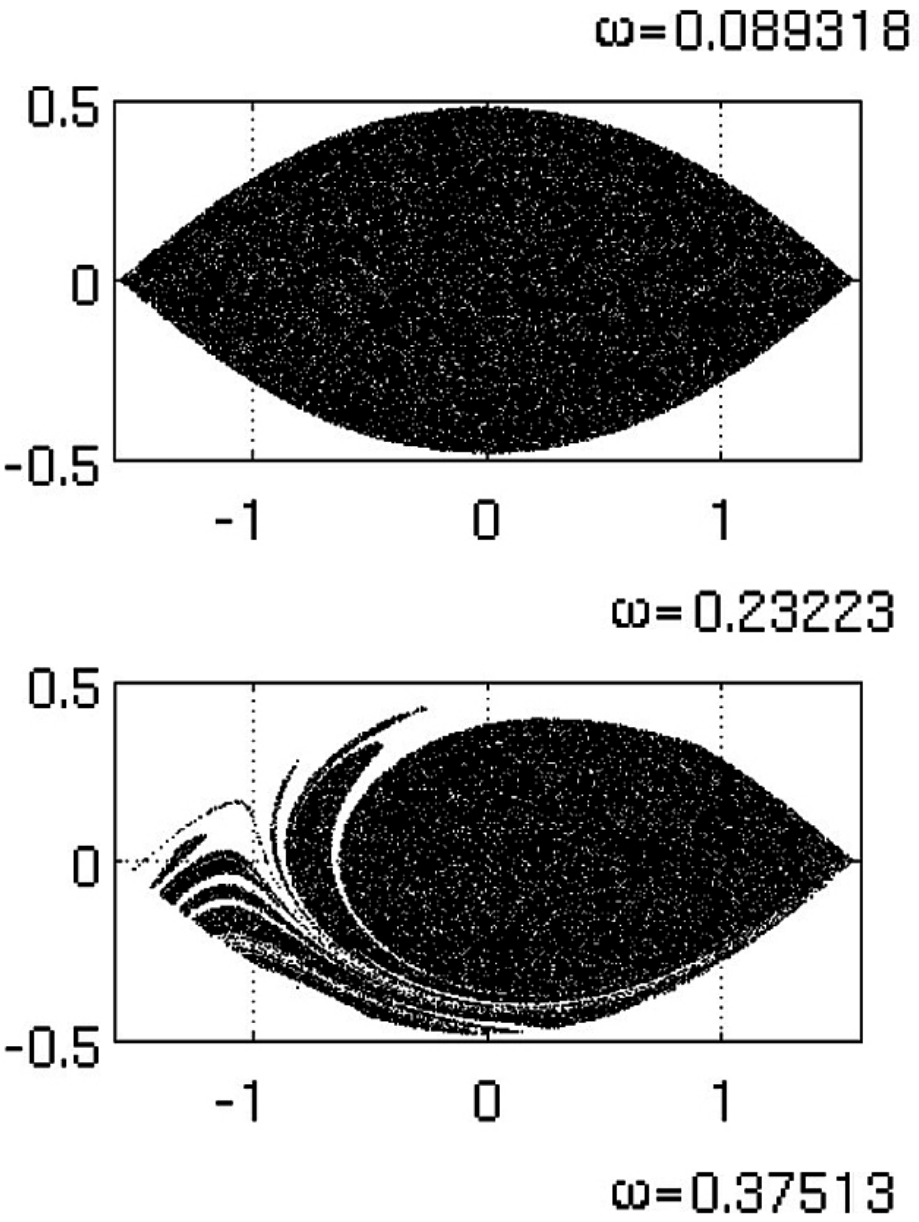

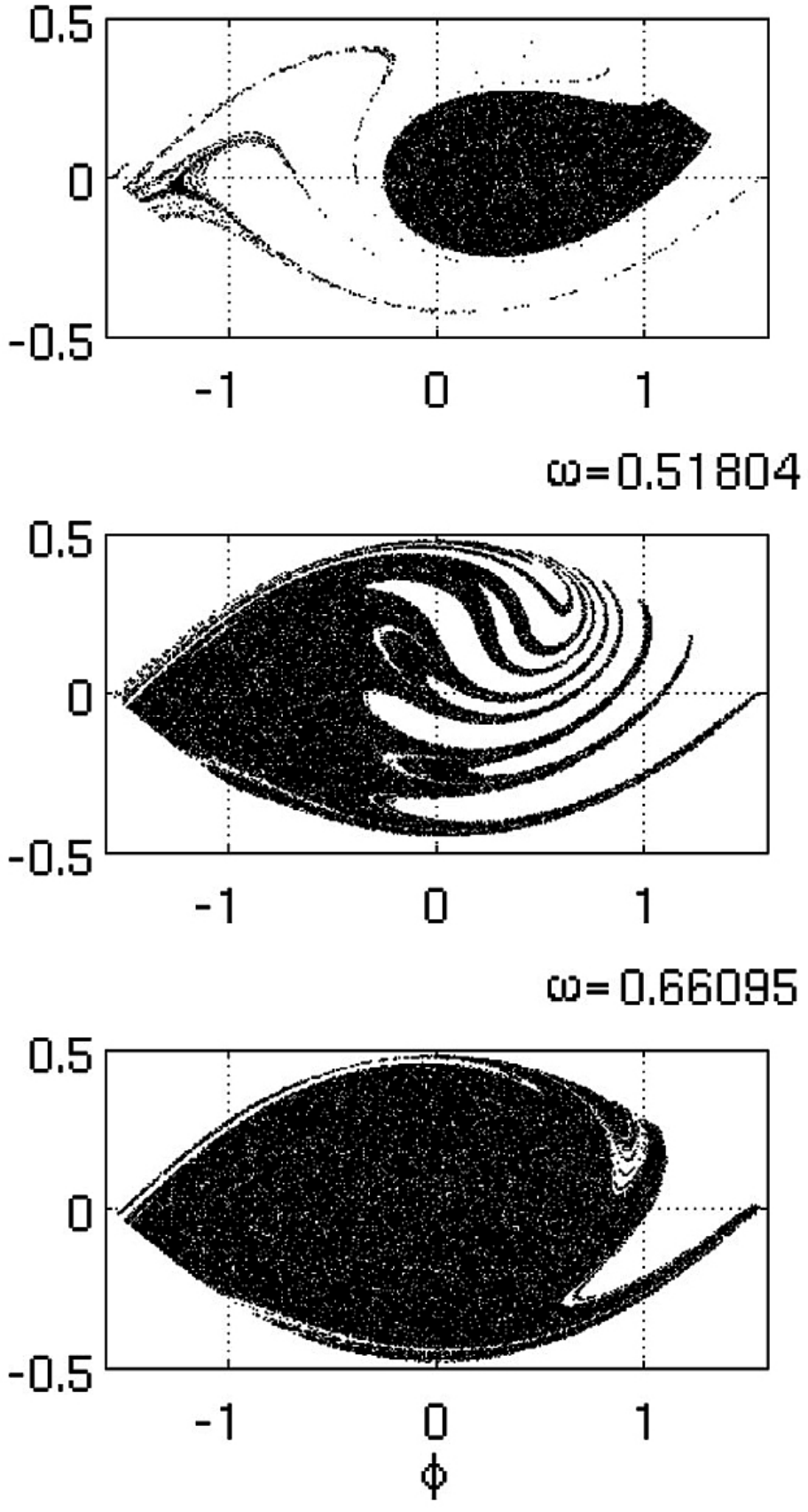

fields along the coordinate axes x, y, z, respectively. One can clearly see that the erosion phenomenon is more emphasized for AC field polarization along the intermediate anisotropy axis y of

the particle, where it almost reaches over 70%, while field polarizations along x and z produce a maximum degree of erosion of 25% and 20%, respectively. This is consistent with analytical predictions given by Eq. (8) for the onset of the heteroclinic tangle. In fact, by looking at Fig. 2, one can see that, for a sufficiently large AC field amplitude h_{ac}, there exist a range of ω such that a chaotic dynamics region is created. Moreover, one can see that, for any polarization of the AC field, there is always an upper bound on the frequency which sustains the existence of such chaotic region. If

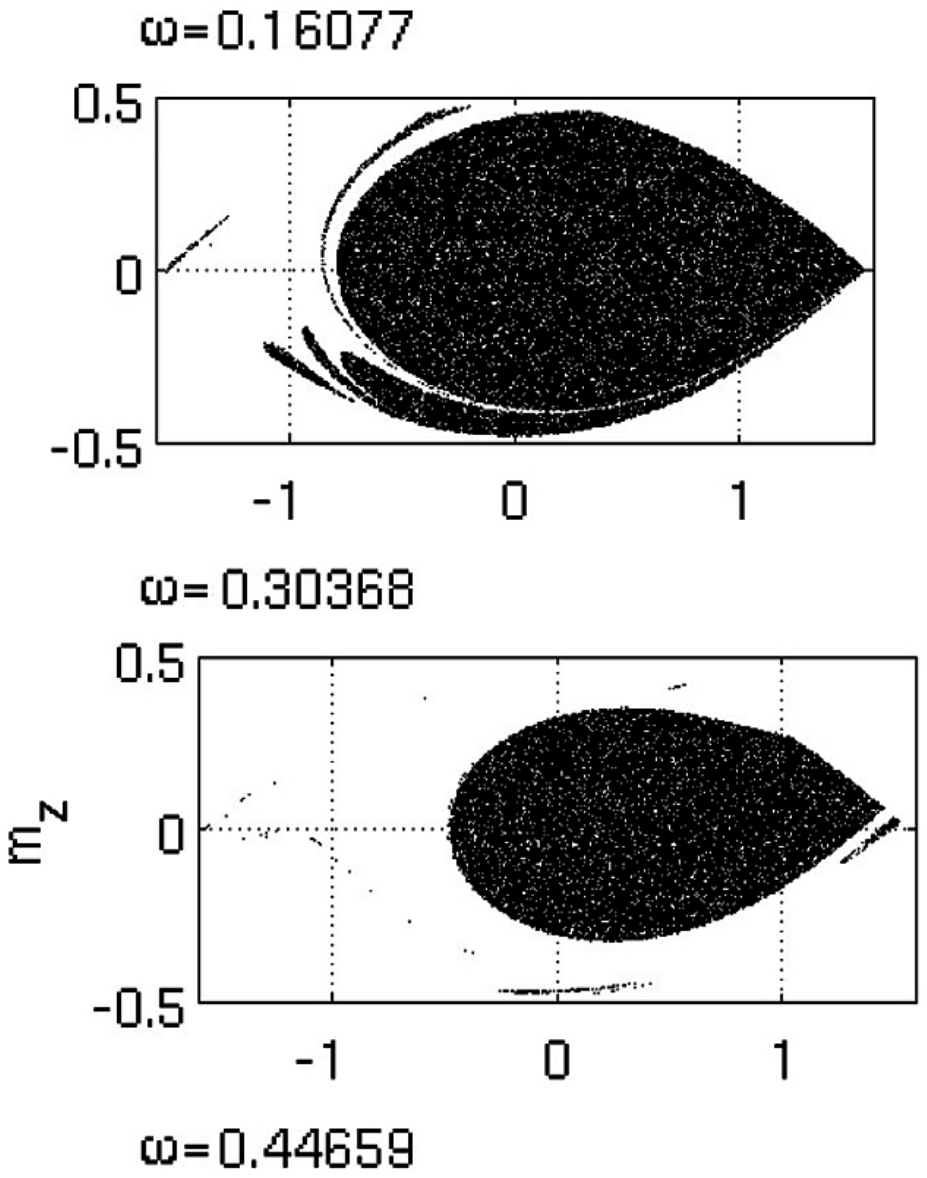

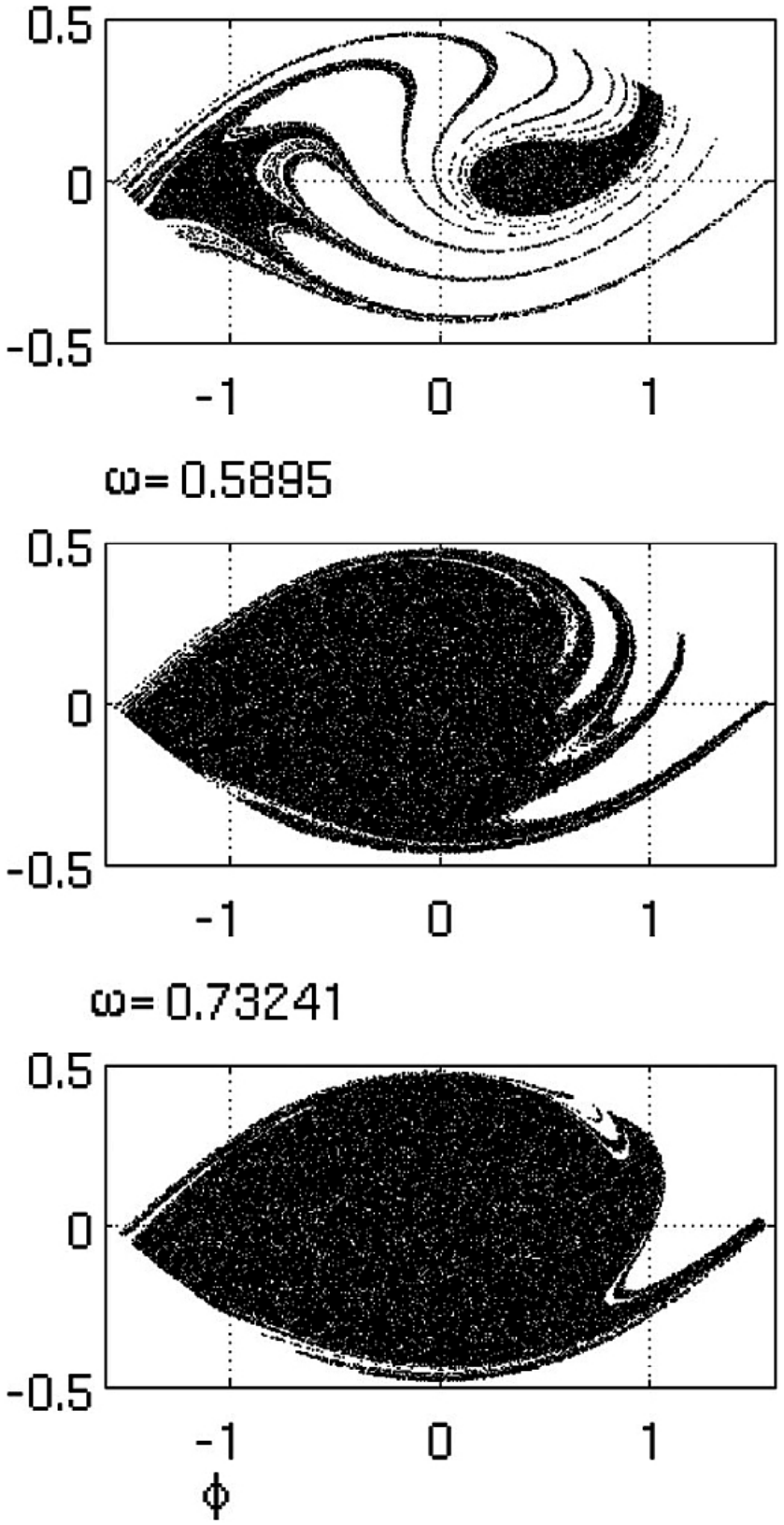

Fig. 4. Basin erosion produced for fields linearly polarized along y direction. The figures show the region $-\pi/2 \leq \phi \leq \pi/2$ and $-0.5 \leq m_z \leq 0.5$ of the (m_z, ϕ)-plane. The low energy well is initially filled by $N = 10^5$ phase points. When the trajectory originating from a phase point escapes the well within the 5 iterations of the stroboscopic map, it is considered 'unsafe' and disregarded. The phase point remaining in the well correspond to 'safe' initial conditions. Values

of parameters: $D_x = -0.3$, $D_y = 0$, $D_z = 1$, $\alpha = 0.01$, and $h_{ac} = 0.05$.

one starts increasing ω from moderately low frequency, it is expected that the degree of erosion increases but, according to Eq. (8) and Fig. 2, this behavior should not be monotone owing to the existence outlined above an upper bound for the frequency supporting the heteroclinic tangle.

As a consequence, the behavior of the degree of erosion η in Fig. 3 resembles that of a resonant frequency response of the particle to the AC field. We immediately observe that such response exhibits peaks well below the Kittel frequency $\sqrt{(D_y - D_x)(D_z - D_x)} = 0.62$ associated with the stable equilibria $m_x = \pm 1$. One can also notice that, for small AC field amplitude, the response η exhibits a single peak, whereas as far as the AC power is increased, multiple peaks appear which cannot be explained by simple perturbation techniques.

In order to deeply understand the mechanism behind basin erosion, we have studied the iterates of the stroboscopic map as function of ω. The result is visible in Fig. 4, where the case of field polarization along the y-axis is considered. It is apparent that, for intermediate frequency values, a complexly shaped region (white region in Fig. 4) traverses the energy well from left to right. Such region exhibits a finely entangled structure which is the signature of fractal basin boundaries produced by the intersection of stable and unstable manifolds of the strobosopic map, as mentioned before.

Finally, it is worth observing that there will be frequency ranges for which the initial magnetization states approximately along the x-axis will be destabilized by the AC excitation, producing the escape from the potential well. This mechanism can explain what is observed for microwave assisted magnetization switching in the presence of a DC applied field [10,11].

In this respect, it is expected that the phenomena analyzed in

this paper may be relevant in the area of energy assisted magnetization switching.

Acknowledgments

This work was partially supported by MIUR-PRIN Project #2010ECA8P3 DyNanoMag.

References

[1] P.E. Wigen (Ed.), Nonlinear Phenomena and Chaos in Magnetic Materials, World Scientific Publishing, Singapore, 1994.
[2] C. Kittel, Phys. Rev. 73 (1948) 155.
[3] D.J. Seagle, S.H. Charap, J.O. Artman, J. Appl. Phys. 57 (1965) 15.
[4] J.M.T. Thompson, Proc. R. Soc. Lond. A 421 (1989) 195.
[5] J. Guckenheimer, P. Holmes, Nonlinear Oscillations, Dynamical Systems, and Bifurcations of Vector Fields, Springer, New York, 1986.
[6] G. Bertotti, I.D. Mayergoyz, C. Serpico, Nonlinear Magnetization Dynamics in Nanosystems, Elsevier, Amsterdam, 2009.
[7] E. Ott, Chaos in Dynamical Systems, Cambridge University Press, New York, 1993.
[8] C. Serpico, A. Quercia, G. Bertotti, M. d'Aquino, I. Mayergoyz, S. Perna, P. Ansalone, J. Appl. Phys. 117 (2015) 17B719.
[9] C. Thirion, W. Wernsdorfer, D. Mailly, Nat. Mater. 2 (2003) 524.
[10] M. d'Aquino, C. Serpico, G. Bertotti, I.D. Mayergoyz, R. Bonin, IEEE Trans. Magn. 45 (2009) 3950–3953.
[11] M. d'Aquino, G. di Fratta, C. Serpico, G. Bertotti, R. Bonin, I.D. Mayergoyz, J. Appl. Phys. 109 (2011) 07D349.